



INSTITUT DE FRANCE  
Académie des sciences

# *Comptes Rendus*

---

# *Physique*

Pierre Touboul, Gilles Métris, Manuel Rodrigues, Yves André  
and Alain Robert

**The MICROSCOPE space mission to test the Equivalence Principle**

Volume 21, issue 2 (2020), p. 139-150.

<<https://doi.org/10.5802/crphys.24>>

**Part of the Thematic Issue:** Prizes of the French Academy of Sciences 2019

© Académie des sciences, Paris and the authors, 2020.  
*Some rights reserved.*

 This article is licensed under the  
CREATIVE COMMONS ATTRIBUTION 4.0 INTERNATIONAL LICENSE.  
<http://creativecommons.org/licenses/by/4.0/>



*Les Comptes Rendus. Physique* sont membres du  
Centre Mersenne pour l'édition scientifique ouverte  
[www.centre-mersenne.org](http://www.centre-mersenne.org)



---

Prizes of the French Academy of Sciences 2019 / *Prix 2019 de l'Académie des sciences*

# The MICROSCOPE space mission to test the Equivalence Principle

*La mission spatiale MICROSCOPE pour le test du Principe d'Equivalence*

Pierre Touboul<sup>a</sup>, Gilles Métris<sup>\*, b</sup>, Manuel Rodrigues<sup>a</sup>, Yves André<sup>c</sup>  
and Alain Robert<sup>d</sup>

<sup>a</sup> ONERA, Université Paris Saclay, Chemin de la Hunière, BP 80100, F-91123 Palaiseau Cedex, France

<sup>b</sup> Université Côte d'Azur, Observatoire de la Côte d'Azur, CNRS, IRD, Géoazur, 250 avenue Albert Einstein, F-06560 Valbonne, France

<sup>c</sup> CNES, 18 avenue Edouard Belin, F-31401 Toulouse, France

*E-mails:* pierre.touboul@onera.fr (P. Touboul), gilles.métris@oca.eu (G. Métris), manuel.rodrigues@onera.fr (M. Rodrigues), yves.andre@cnes.fr (Y. André), AlainJM.Robert@cnes.fr (A. Robert)

**Abstract.** The MICROSCOPE space experiment aimed to test the Equivalence Principle with a much better accuracy than ever before. Its principle is to compare the free fall of concentric test masses embedded in a space accelerometer onboard a satellite orbiting the Earth. The effect of non-gravitational forces on the motion of the satellite is strongly reduced thanks to the so-called drag-free system. MICROSCOPE ran from April 2017 until October 2019. The analysis of the first series of measurements leads to an improvement of about an order of magnitude on the accuracy of the test of the Equivalence Principle. No violation has been detected for the pair of masses in platinum and titanium at the level of  $10^{-14}$ .

MICROSCOPE, proposed by ONERA and OCA as science leaders and developed by CNES as project manager, is the first European space mission dedicated to fundamental physics on low Earth orbit. ZARM, PTB and ESA are the main European contributors.

**Résumé.** La mission spatiale MICROSCOPE avait pour objectif de tester le Principe d'équivalence (PE) avec une précision bien meilleure que ce qui avait été fait jusqu'alors. Ce type de test a un enjeu important car, tandis que le PE est un pilier de la relativité générale, il n'est pas imposé par la plupart des théories alternatives visant à étendre la gravitation pour l'unifier avec les autres interactions de la physique. Fondamentalement l'expérience consiste à comparer les chutes libres de différentes masses. Pour des raisons de mise en œuvre, le mouvement des masses n'est pas libre mais contrôlé par un accéléromètre (la charge utile du satellite) et c'est la force électrostatique nécessaire à maintenir les masses au repos qui constitue la mesure. Plus précisément, on compare les forces par unité de masse exercées sur des masses concentriques et on recherche dans leur différence la signature d'une différence de comportement vis-à-vis de la gravité terrestre. L'avantage d'un

---

\* Corresponding author.

test dans l'espace est de permettre une chute quasi-infinie et de minimiser de nombreuses perturbations environnementales. Le satellite est équipé de micro-propulseurs dont les poussées sont asservies pour d'une part contrebalancer les forces non-gravitationnelles et d'autre part maintenir une loi d'attitude très stable.

Le satellite MICROSCOPE a été lancé en avril 2016 et a fonctionné avec succès jusqu'en octobre 2018, date à laquelle sa passivation a été réalisée. De nombreuses sessions de mesures ont été réalisées, non seulement pour faire le test du PE dans différentes conditions mais aussi pour caractériser l'expérience et étalonner les instruments. Les analyses de l'ensemble des données est en cours de finalisation, mais les résultats obtenus à partir des toutes premières sessions de mesure apportent déjà un progrès important par rapport à l'état de l'art : une seule session de mesure a permis d'améliorer la précision du test d'un ordre de grandeur, concluant à l'absence de violation du PE pour le couple de matériaux platine-titanium, au niveau de  $10^{-14}$ . Une autre session de mesure comparant 2 masses de mêmes compositions (platine) a permis de vérifier l'absence de systématismes importants dans l'expérience puisque : aucune violation supérieure à  $10^{-14}$  n'a été détectée.

**Keywords.** Equivalence principle, Space experiment, Satellite, Accelerometers, Drag free, Inertial mass, Gravitational mass.

**Mots-clés.** Principe d'équivalence, Expérience spatiale, Satellite, Accéléromètres, Compensation de trainée, Masse inertielle, Masse gravitationnelle.

**2020 Mathematics Subject Classification.** 83B05.

## 1. Introduction

At the beginning of the 17th century, as part of his work on falling bodies based on the observation of the descent of different balls on inclined planes, Galileo noted that these movements were identical regardless of the size and material composition of these bodies [1]. This result, in apparent contradiction with daily experience, was obtained thanks to the virtual elimination of the main non-gravitational disturbance constituted by dragging by the atmosphere and which affects bodies differently according to their cross section and their mass. Half a century later, Newton confirmed this universality of free fall by comparing the beatings of pendulums with various test masses and presented this universality as a consequence of the law of gravitation and Newton's second law [2]: the first states that the force of gravity which attracts bodies to each other is proportional to their mass (called gravitational in this case)  $m_G$ ; the second also asserts that the resistance of a body to a modification of its movement (acceleration) by a given force is proportional to its inertial mass  $m_I$ . Therefore the acceleration resulting from the gravitational attraction is proportional to the ratio  $m_G/m_I$ :

$$F = G \frac{m_G m_G}{r^2} \quad \text{and} \quad a = \frac{F}{m_I} \implies a = \frac{G M_G}{r^2} \frac{m_G}{m_I}. \quad (1)$$

Newton was well aware that these two concepts of mass were very different but the experimental verification of the universality of free fall led to the conclusion that the ratio  $m_G/m_I$  is the same for all bodies: the gravitational and inertial masses are proportional or equivalent. This equivalence is generally quantified by the Eötvös parameter:

$$\eta(A, B) = \frac{\frac{m_{G,A}}{m_{I,A}} - \frac{m_{G,B}}{m_{I,B}}}{\frac{1}{2} \left( \frac{m_{G,A}}{m_{I,A}} + \frac{m_{G,B}}{m_{I,B}} \right)} = \frac{a_A - a_B}{\frac{1}{2} (a_A + a_B)}. \quad (2)$$

The equivalence was checked more and more precisely in the following centuries to reach  $10^{-9}$  at the turn of the 20th century, thanks to Eötvös' experiments using a torsion balance [3]. An experiment with much more efficient technology is currently running at Washington University in Seattle; it recorded the most precise determination, before MICROSCOPE, of the Eötvös parameter for laboratory bodies: they demonstrated that the value of this parameter was compatible

with 0 for the couples (Beryllium, Titanium) and (Beryllium, Aluminium) with order of accuracy of  $2 \times 10^{-13}$  [4]. Another type of experiment consists in comparing the movements (very close to free falls) of different celestial bodies. The most precise experiment of this type consists in comparing the movement of the Moon and the Earth in the gravitational field of the Sun, thanks to the very precise measurement of the Earth–Moon distance by means of laser telemetry [5]. For such massive bodies, another focus, in addition to a possible violation due to different compositions of the bodies, is the search for a violation related to the self-gravitational energy of the bodies (Nordvedt effect) [6]. The best result was obtained by [7]. The two types of experience are therefore highly complementary.

In 1907 Albert Einstein defined the Equivalence Principle (EP) [8] which is one of the pillars of his theory of gravitation, General Relativity (GR) [9]. The equivalence of the gravitational and inertial masses as well as the universality of free fall are consequences of the EP. GR has led to many new predictions which have all been verified since, such as for example the existence of black holes and gravitational waves confirmed in 2016 [10]. It remains, however, to unify the theory of gravitation, relevant to large scales, with quantum mechanics relevant to small scales. There are several theories seeking to fulfil this objective and, unlike GR, they most often allow a violation of the EP [11]. Thus, experiments that are able to detect whether or not the EP has been violated with a greater degree of precision, bring important landmarks for these theories.

Ground based experiments as cited above are limited by the disturbing environment or by the duration of the experiment. In space far from Earth vibrations and day/night temperature variations, and with much more measurement time, it is possible to compensate for the external disturbing forces and torques in order to provide the best environment ever in a low Earth orbit.

The first idea of an EP test in space was first proposed in the 1970's [12] and studied at the end of the 20th century at Stanford University [13] with the STEP mission. STEP comprised cylindrical accelerometers with electrostatic control for the start-up and SQUID detectors for the fine test-mass position measurement. STEP was a complex cryogenic mission proposal with an expected accuracy of  $10^{-18}$  on the EP test. Taking advantage of the Myriade line of CNES micro-satellite, MICROSCOPE appeared at the beginning of the 21st century to be a simpler and quicker mission with an objective of testing the EP at the level of  $10^{-15}$  [14,15], already a breakthrough with respect to current results.

In this paper we present the first space experiment which aims at testing the EP. The principle of the mission is described in Section 2 while brief descriptions of the satellite and of the instrument are presented in Sections 3 and 4. The very first results of the mission are summarised in Section 5.

## 2. The MICROSCOPE mission

MICROSCOPE aimed to test the Equivalence Principle with an unprecedented precision of  $10^{-15}$ . The T-SAGE (Twin Space Accelerometers for Gravitation Experiment) scientific payload, provided by ONERA, was integrated within a CNES micro-satellite. It was launched and injected into a 710 km altitude, circular orbit, by a Soyuz launcher from Kourou on April 25, 2016. The orbit is sun-synchronous, dawn-dusk (i.e. the ascending node stays at 18h mean solar time) in order to have long eclipse-free periods (eclipses are defined as periods within the Earth's shadow and happen only between May and July).

In the spirit, the experiment aims to compare the free fall of several test masses orbiting the Earth. But, for practical reasons, the implementation is slightly more sophisticated and relies on two nested control loops.

The first loop is inside the payload T-SAGE constituted by 4 test masses grouped by pairs in two differential accelerometers. Each test mass is placed between pairs of electrodes and its motion

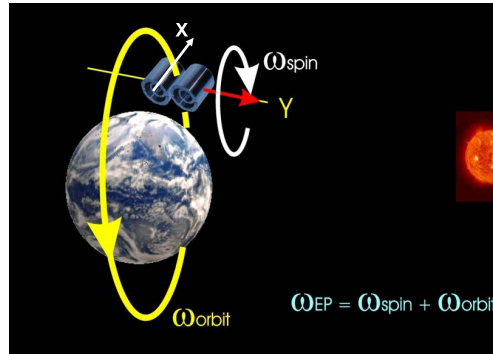


**Figure 1.** Configuration of the experiment: the most sensitive axis  $x$  (along the axis of the cylinders) of the accelerometers is maintained parallel to the orbital plane and rotates around the axis normal to the orbit.

with respect to its cage fixed to the satellite is monitored by capacitive sensors. This motion can then be controlled at rest by applying the appropriate electrostatic force calculated by a PID (Proportional Integral Derivative). This means that this electrostatic force compensates for all other forces. In that way, knowledge of the applied electrostatic potential allows us to measure the acceleration which would affect the test mass with respect to the satellite in the absence of the electrostatic force. That is why, in the following, we will use the terminology “measured acceleration” even if the masses are motionless with respect to the satellite.

The other major control loop in the MICROSCOPE experiment is included in the Drag-Free and Attitude Control System (DFACS) which applies accelerations on the satellite in order to cancel (or at least to considerably reduce), the level of the common mode measured acceleration. This is achieved by means of cold gas thrusters. This system also ensures a very accurate control of the pointing as well as the angular velocity and acceleration based on the measurements of angular position delivered by the stellar sensors and of the angular acceleration delivered by T-SAGE.

Even if T-SAGE measures the linear acceleration along the 3 axes, the measurement along the  $x$ -axis, which is also the axis of the cylindrical test masses, is the most accurate. This axis is controlled, thanks to the DFACS, parallel to the orbital plane and rotates with a frequency  $f_{\text{spin}}$  around the  $y$ -axis orthogonal to the orbital plane (Figure 1). In these conditions the component  $g_x$  of the Earth's gravity, and then the searched EP signal  $\eta g_x$ , varies with a very stable frequency  $f_{\text{EP}} = f_{\text{orb}} + f_{\text{spin}}$  where  $f_{\text{orb}}$  is the mean orbital frequency.

At first view, the main perturbation comes from the Earth's gravity gradient, due to the fact that, despite our best efforts in terms of manufacturing, the centres of mass of the test masses are not located in exactly the same place, but are separated by an off-centering  $\vec{\Delta}$  of a few tens of micrometers. At the altitude of MICROSCOPE this leads to a differential acceleration of a few  $10^{-11} \text{ m}\cdot\text{s}^{-2}$ , much larger than the accuracy of  $10^{-15} \times (7.9 \text{ m}\cdot\text{s}^{-2}) = 7.9 \times 10^{-15} \text{ m}\cdot\text{s}^{-2}$  targeted for the EP signal. But thanks to the careful design of the experiment (orbit close to circular, sensitive axis maintained in the orbital plane) this gravity gradient signal is mainly concentrated at DC and  $2 f_{\text{EP}}$  frequencies and well decorrelated from the EP signal. Moreover, the component  $\Delta_y$  has a fully negligible impact whereas the components  $\Delta_x$  and  $\Delta_z$  can be accurately estimated in flight and the corresponding terms of the gradient can be corrected [16].

Up to negligible correcting terms, the model of the measured acceleration takes the simple form:

$$\Gamma_{x,\text{corr}}^{(d)} = b_x^{(d)} + \delta_x g_x + \Delta_x S_{xx} + \Delta_z S_{xz} + k_x^{(d)} \Gamma_x^{(c)} + \theta_z^{(d)} \Gamma_y^{(c)} + \theta_y^{(d)} \Gamma_z^{(c)} + n_x^{(d)}, \quad (3)$$

where

- $\Gamma_{x,\text{corr}}^{(d)}$  is the difference of the accelerations measured for the two quasi-concentric test masses along the  $x$ -axis,
- $b_x^{(d)}$  is the differential bias, mainly constant but also potentially including low frequency thermal effects,
- $\delta_x$  is very close to the Eötvös parameter  $\eta$ ,
- $g_x$  is the gravity acceleration projected along the  $x$ -axis,
- $\Delta_x$  and  $\Delta_z$  are the components along  $x$  and  $z$  respectively, of the vector separating the two test masses,
- $S_{xx}$  and  $S_{xz}$  are components of the gradient of acceleration along  $x$  due to differences of position along  $x$  and  $z$  respectively:  $S_{xx} = T_{xx} + \Omega_y^2 + \Omega_z^2$  and  $S_{xz} = T_{xz} - \Omega_x \Omega_z$  where  $[T]$  is the gravity gradient tensor (the space derivative of the gravity acceleration) and  $\vec{\Omega}$  is the angular velocity of the satellite,
- $\tilde{\Gamma}^{(c)}$  is the common mode applied acceleration residue when the DFACS is operating,
- $k_x^{(d)}$  is the difference of scale factor related to the measurement process for the two test masses,
- $\theta_y$  and  $\theta_z$  are the test mass relative misalignment around  $y$  and  $z$ ,
- $n_x^{(d)}$  is the differential noise.

$g_x$ ,  $S_{xx}$  and  $S_{xz}$  can be computed very accurately from the known position and attitude (i.e. the orientation in space) of the satellite, whereas  $b_x^{(d)}$ ,  $\delta_x$ ,  $\Delta_x$  and  $\Delta_z$  are parameters estimated during the data analysis process [17]. The common mode acceleration effect is also corrected thanks to calibration sessions which allow us to estimate  $k_x^{(d)}$ ,  $\theta_y$  and  $\theta_z$ .

### 3. The satellite and the acceleration and attitude control system

#### 3.1. Satellite design

The MICROSCOPE satellite was designed and developed by CNES as a space laboratory devoted to test the Equivalence Principle. The satellite points the instrument accurately along 3 directions, protects it against non-gravitational forces, and ensures an ultra-stable thermal and gravitational environment, with a very low level of microphonic or micro-acceleration disturbances. It is in close interaction with its payload, the science instrument developed by ONERA described in Section 4.

The satellite was derived from the Myriade micro-satellite product line and its architecture was based on DEMETER [18] and PARASOL, the first satellites of the Myriade family [19]. But the design of MICROSCOPE was extensively adapted for this mission (Figure 2).

The first design driver was the reduction of the mean level of applied accelerations on the instrument introducing a new function: the acceleration control (currently named drag-free control) [20]. This function uses the payload as an inertial sensor to measure the external forces.

The acceleration control is performed by the cold gas micro propulsion system (provided by ESA), which allows us to counteract the perturbations (atmospheric drag, radiation pressure, electromagnetic forces) at a very small level of tens of  $\mu\text{N}$ . The combination of the six degrees of freedom (angular and linear acceleration) enables the control of torques and forces in a single subsystem, called DFACS.

The thermal and mechanical architecture design was driven by the need to centre the instrument as close as possible to the satellite centre of mass and by the high thermal stability requirement around  $f_{EP}$ : better than 1 mK at the sensor unit interface and 10 mK at the associated analog electronics interface. Therefore, these most thermally sensitive payload units have been integrated in a specific cocoon at the core of the satellite structure: the BCU, the payload box.

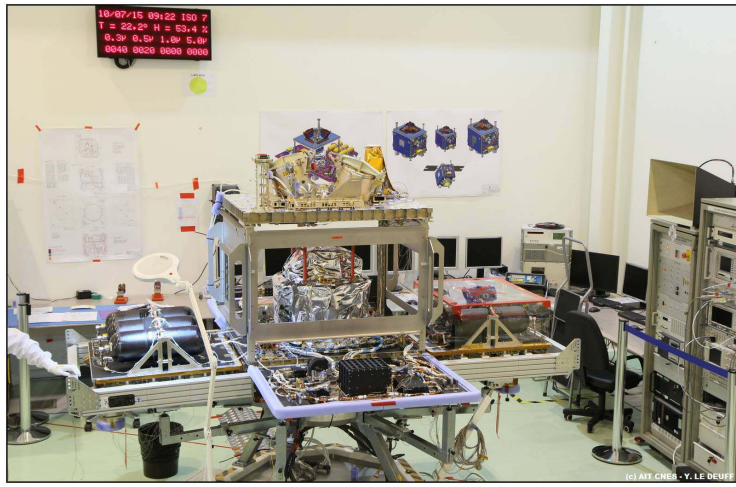


**Figure 2.** (© AIT-CNRS Y. Le Deuff). The MICROSCOPE satellite being integrated. This is a space laboratory of about 300 kg. Once closed, the shape is of a cube measuring  $1.4 \text{ m} \times 1 \text{ m} \times 1.5 \text{ m}$ . We distinguish in particular the payload T-SAGE (at the centre, under the silver coating), and the micro-propulsion  $2 \times 3$  tanks (on the left and right walls), carrying 16 kg of gas under a pressure of 400 bar at the beginning of life.

For the other Myriade satellites, the payload was located on top of the platform and the tank of the propulsion system was at the centre. The need to ensure an ultra-stable thermal and gravitational environment, with a very low level of microphonic or micro-acceleration disturbances, imposed a lot of constraints in terms of conception, component selection, manufacturing and integration.

### 3.2. The attitude and acceleration control subsystem

The diagram of the DFACS operation principle is shown in Figure 3. The satellite must protect the payload and thus the test masses from all non-gravitational forces perturbing the EP test experiment and so an active control of the acceleration and of the attitude of the satellite has been implemented. The performance of the overall mission was evaluated taking into consideration all subsystems. To specify the DFACS and the payload in close link was a real challenge.

The DFACS in orbit performance exceeded expectations. Some results are summarised here. The common acceleration of the spacecraft was reduced to much better than the specified  $10^{-12} \text{ m} \cdot \text{s}^{-2}$  around the EP test frequency  $f_{\text{EP}}$ , see Figure 4. Around twice this frequency, the specification is relaxed by a factor 3 to 10, sufficient to estimate the Earth's gravity gradient effect and thus to calibrate the off-centring of the pair of concentric test masses. This control had to deal with non-gravitational accelerations (atmospheric braking and radiation pressure) leading to a mean common mode acceleration signal greater than  $10^{-8} \text{ m} \cdot \text{s}^{-2}$ .

At  $f_{\text{EP}}$ , the angular pointing is controlled to less than 7  $\mu\text{rad}$  with an angular velocity stability better than  $10^{-9} \text{ rad} \cdot \text{s}^{-1}$  and the angular acceleration better than  $10^{-11} \text{ rad} \cdot \text{s}^{-2}$ . This function needs a very sensitive 6-axis sensor and very fine actuators. For this reason, the accelerometers, which are also able to measure angular accelerations, are used as the main sensor of the DFACS control loop with a priori onboard correction of the scale factor to better than 5% and of the biases to better than a few percent. Scale factors matching is better estimated to an accuracy of a few

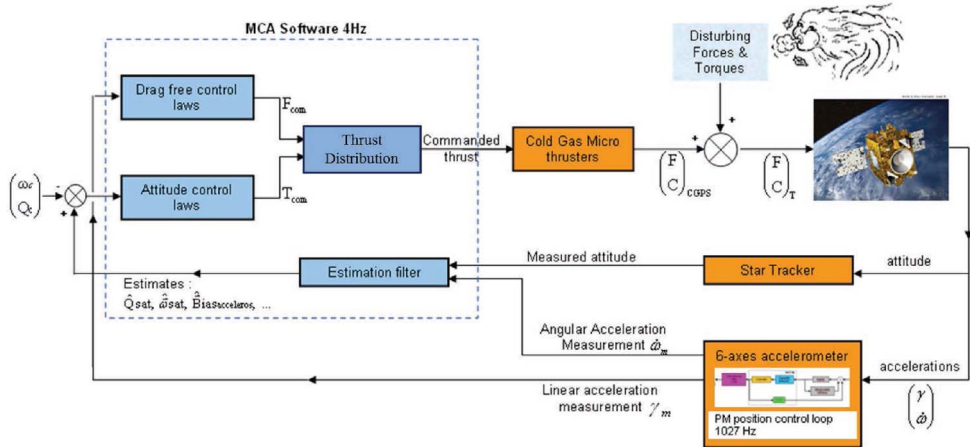


**Figure 3.** DFACS control loop schematic diagram.

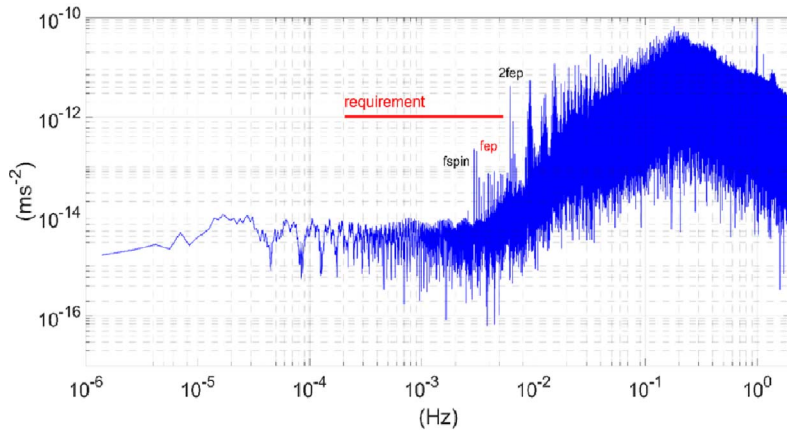


**Figure 4.** Discrete Fourier Transform of the measured acceleration on the drag-free sensor along X axis.

$10^{-5}$  in dedicated calibration sessions to correct the measurements in the scientific data process: indeed the onboard DFACS needs only rough estimations. The choice of the test mass reference in the drag-free loop was defined by the scientific needs at each session. Estimated attitude is the result of the hybridisation between the attitude measurements provided by the Star Trackers and the angular accelerations measured by T-SAGE. The control laws for the acceleration and the attitude servo-loops define the total forces  $F_{\text{com}}$  and torques  $T_{\text{com}}$  (Figure 3) to be applied on the satellite to compensate for the external perturbations. The commanded forces and torques are transformed into 8 thrust orders sent to the Cold Gas Propulsion System (CGPS).

#### 4. The science instrument

The satellite comprises only one payload: T-SAGE (Twin-Space Accelerometers for Gravity Experiment). T-SAGE was designed on the legacy of more than 40 years' experience of developing electrostatic accelerometers [21] which provided the best means of mapping the Earth's gravity

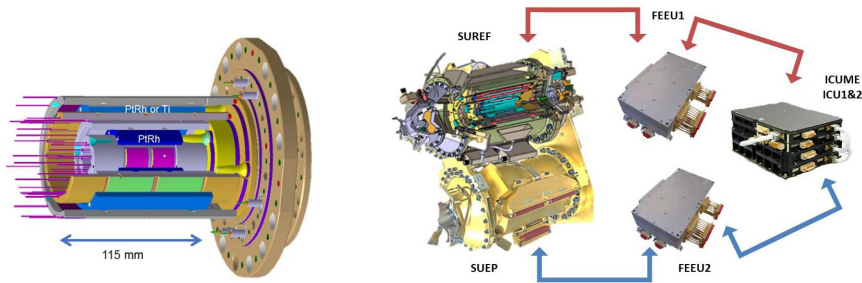


**Figure 5.** Diagram of T-SAGE. Left: cross-section of one SU with the pair of concentric test masses surrounded by a set of 4 cylinders carrying the electrodes. Right: the two SUs, the two FEEUs and the two ICUs stacked into one unit called ICUME.

field: GRACE [22], GOCE [23, 24]. The payload is composed of two sensor units (SU), see Figure 5, each one associated with very accurate analog electronics (Front End Electronic Unit, FEEU) and a digital electronic unit for the test-mass servo-loop and communication with the satellite (Interface Control Unit, ICU). It operates at room temperature and is based on full electrostatic accelerometers.

Two concentric and cylindrical test masses in each SU define the accelerometer core. The SU using two test masses made of two different materials, platinum–rhodium alloy for one and titanium alloy for the other, is called SUEP and is used to test the WEP. The other SU with both test masses made of platinum–rhodium alloy serves as a reference to check the whole experiment and gives more weight to the SUEP results. Each test mass is surrounded by a set of electrodes (Figure 5) that provides a 100 kHz capacitive detection of its motion which is converted in the FEEU into a DC voltage proportional to the displacement at first order. The detection signal is entered at the input of a 40-bit digital controller in the ICU, based on a PID (Proportional Integral Derivative) servo-loop. The output of the PID is representative of the test mass degrees of freedom acceleration and transmitted to the spacecraft onboard computer (OBC).

The stability of the accelerometric measurement [17] is mainly obtained thanks to the very accurate reference voltage applied to the test-mass through a thin gold wire of 7  $\mu\text{m}$ . This DC voltage,  $V_p$  (in Figure 6), determines at first order the scale factor of the instrument when opposite voltages are applied to opposite electrodes of one degree of freedom. However, the gold wire damping introduces a Nyquist noise [25], which constitutes the performance limit for this type of accelerometer.

In order to perform the EP test in the best accelerometric environment conditions, the OBC picks up the outer test mass measurements and calculates the necessary thrusts to be applied on each thruster to nullify the accelerometer outputs. The disturbing forces (air drag and solar pressure) and torques (magnetic and gravitational) felt by the satellite are thus taken into account and counteracted. The scientific data process calculates the difference of the measured acceleration in order to extract the Eötvös parameter. After a few months of operation, the differential acceleration noise was established to be quite stable and evaluated to less than  $2 \times 10^{-11} \text{ m}\cdot\text{s}^{-2}\cdot\text{Hz}^{-1/2}$  at  $f_{\text{EP}} = 0.9 \times 10^{-3} \text{ Hz}$  for the SUREF and to less than  $5 \times 10^{-11} \text{ m}\cdot\text{s}^{-2}\cdot\text{Hz}^{-1/2}$  at  $f_{\text{EP}} = 3 \times 10^{-3} \text{ Hz}$  for the SUEP.

## 5. First results

The MICROSCOPE mission is divided into different measurement sessions. Sessions represent a time span during which the satellite and the instrument keep the same configuration (spin, drag-

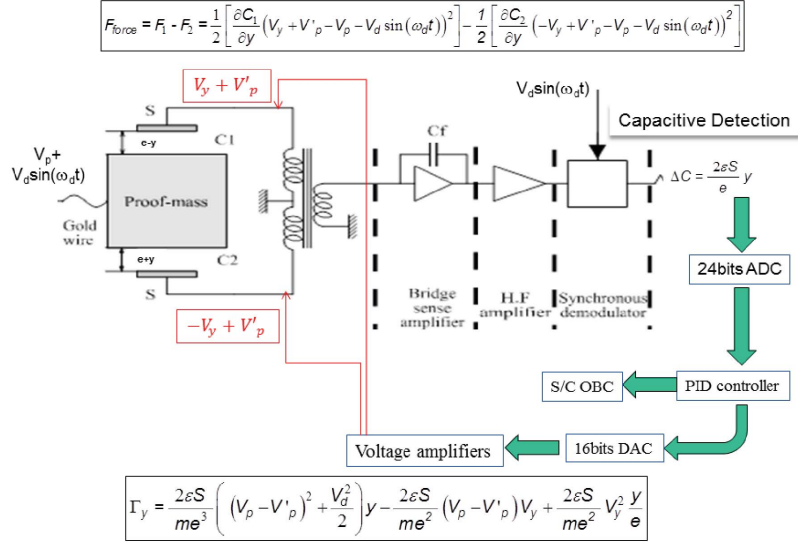


**Figure 6.** Schematic of one degree of freedom servo-loop control.

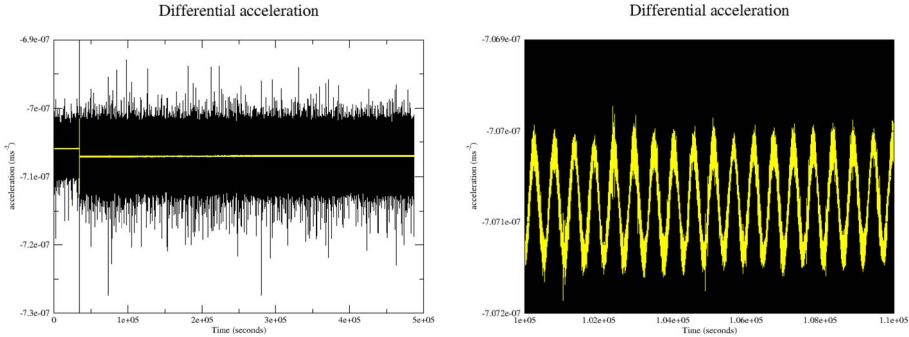


**Figure 7.** Differences in the accelerations measured along the X-axis, between the two test masses of the SUREF instrument. Raw data (black) and after a running average over 240 points (yellow). The zoom on the averaged data (right panel) highlights the periodic signal due to the gravity gradient.

free control law etc.). Some of these sessions are directly devoted to the EP test while others are used to calibrate or characterise the experiment. EP sessions are the longest, most of them lasting 120 orbital periods (about 8 days), while calibration sessions typically last a few orbits. Figures 7 and 8 show the differential acceleration measured during 2 EP sessions that were among some of the first to take place at the end of the commissioning phase: one session using the instrument SUEP and one session using the instrument SUREF.

The SUREF session had a total duration of 82 orbits, but the precise attitude is available only for the last 62 orbits which limits the analysis to this period. For this session, the spin frequency of the satellite was  $f_{\text{spin2}} = 7.568 \times 10^{-4}$  Hz leading to an EP frequency (the frequency at which the Earth apparently rotates with respect to a frame fixed to the satellite)  $f_{\text{EP}} = 9.249 \times 10^{-4}$  Hz. The

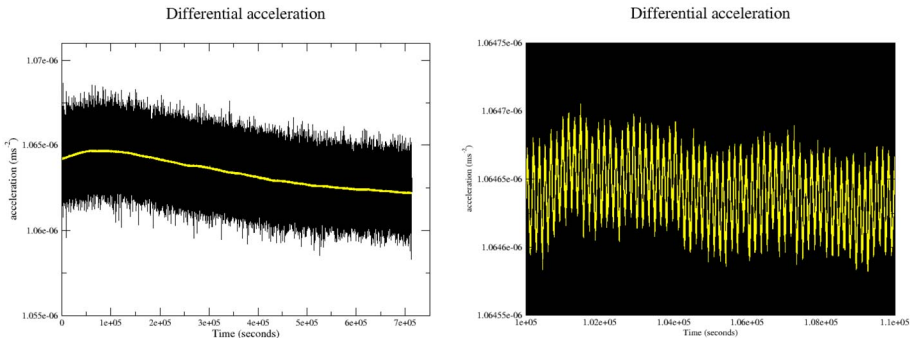


**Figure 8.** Differences in the accelerations measured along the  $X$ -axis, between the two test masses of the SUEP instrument. Raw data (black) and after a running average over 240 points (yellow). The zoom on the averaged data (right panel) highlights the periodic signal due to the gravity gradient.

estimated values of the parameters are [17, 26]:

$$\begin{aligned}\delta &= (4 \pm 4) \times 10^{-15}, \\ \Delta_x &= (-35.39 \pm 0.02) \mu\text{m}, \\ \Delta_z &= (5.55 \pm 0.02) \mu\text{m}.\end{aligned}\quad (4)$$

Note that the above errors are only statistical errors at 1 sigma. A very preliminary and conservative assessment has been conducted for the Eötvös parameter. This leads to [17]

$$\delta(\text{Pt}, \text{Pt}) = [+4 \pm 4(\text{stat}) \pm 8(\text{syst})] \times 10^{-15} \quad (1\sigma \text{ statistical uncertainty}). \quad (5)$$

The SUEP session lasts 120 orbits and the associated spin frequency is  $f_{\text{spin3}} = 2.943 \times 10^{-3}$  Hz leading to the EP frequency  $f_{\text{EP}} = 3.111 \times 10^{-3}$  Hz. The estimated parameters are

$$\begin{aligned}\delta &= (-1 \pm 9) \times 10^{-15}, \\ \Delta_x &= (20.14 \pm 0.05) \mu\text{m}, \\ \Delta_z &= (-5.55 \pm 0.05) \mu\text{m}.\end{aligned}\quad (6)$$

Including the systematic errors we get

$$\delta(\text{Ti}, \text{Pt}) = [-1 \pm 9(\text{stat}) \pm 9(\text{syst})] \times 10^{-15} \quad (1\sigma \text{ statistical uncertainty}). \quad (7)$$

## 6. Conclusion and prospects

Using only one session representing slightly more than eight days of measurement, we have already obtained an accuracy about ten times better than the state of the art before MICROSCOPE. The results are fully compatible with the Equivalence Principle: the free fall of the test masses in platinum and titanium are identical at the  $10^{-14}$  level. Confidence in our results has been strengthened by a double check: first, a very conservative evaluation of the systematic errors leads to an assessment better than  $10^{-14}$  and second, the same experiment conducted with identical test masses in platinum provides a null result with an accuracy better than  $10^{-14}$  [17]. A by-product of this experiment, which is not fundamental but gives a good idea of its level of sensitivity, is the estimation of the distance between the test masses with a precision of a few hundredths of  $\mu\text{m}$  using the induced gravity gradient.

Since then, ten times more sessions have been acquired, both to test the EP and to characterise the whole experiment. This will allow us to improve the statistical error and also the assessment

of systematic errors (articles in preparation). The MICROSCOPE satellite was deactivated in October 2018 and is slowly desorbiting as predicted with the two wings deployed to increase the air braking.

## References

- [1] G. Galilei, *Discours et démonstrations mathématiques concernant deux sciences nouvelles*, Presses Universitaires de France, 1995, French translation by M. Clavelin.
- [2] I. Newton, *Principes mathématiques de la philosophie naturelle*, Librairie scientifique et technique Albert Blanchard, 1966, French translation by la Marquise du Chastellet.
- [3] L. Eötvös, D. Pekár, E. Fekete, "Beiträge zum Gesetz der Proportionalität von Trägheit und Gravität", *Ann. Phys.* **68** (1922), p. 11, English translation in Annales Universitatis Scientiarum Budapestiensis de Rolando Eötvös Nominate, Sectio Geologica, 7, 111, 1963.
- [4] S. Schlamminger, K.-Y. Choi, T. A. Wagner, J. H. Gundlach, E. G. Adelberger, "Test of the equivalence principle using a rotating torsion balance", *Phys. Rev. Lett.* **100** (2008), no. 4, article ID 041101.
- [5] J. Chabé, C. Courde, J.-M. Torre, S. Bouquillon, A. Bourgoin, M. Aimar, D. Albanèse, B. Chauvineau, H. Mariey, G. Martinot-Lagarde, N. Maurice, D.-H. Phung, E. Samain, H. Viot, "Recent progress in lunar laser ranging at grasse laser ranging station", *Earth Space Sci.* **7** (2020), no. 3, article ID e2019EA000785.
- [6] K. Nordtvedt, "Testing relativity with laser ranging to the moon", *Phys. Rev.* **170** (1968), p. 1186-1187.
- [7] V. Viswanathan, A. Fienga, O. Minazzoli, L. Bernus, J. Laskar, M. Gastineau, "The new lunar ephemeris INPOP17a and its application to fundamental physics", *Mon. Not. R. Astron. Soc.* **476** (2018), no. 2, p. 1877-1888.
- [8] A. Einstein, "Über das Relativitätsprinzip und die aus demselben gezogene Folgerunge", *Jahrb. Radioakt Elektronik* **4** (1907), p. 411, English translation in The Collected Papers of Albert Einstein Volume 2, A. Beck and P. Havas (Princeton University Press, 1989) doc.47.
- [9] A. Einstein, "Die Grundlage der allgemeinen Relativitätstheorie", *Ann. Phys.* **354** (1916), p. 769-822.
- [10] B. P. Abbott *et al.*, "Observation of gravitational waves from a binary black hole merger", *Phys. Rev. Lett.* **116** (2016), article ID 061102.
- [11] T. Damour, "Theoretical aspects of the equivalence principle", *Class. Quantum Gravity* **29** (2012), no. 18, article ID 184001.
- [12] P. K. Chapman, A. J. Hanson, "An Eötvös experiment in earth orbit", in *Proc. Conf. on Experimental Tests of Gravitation Theories* (R. W. Davies, ed.), vol. JPL TM 33-499, California Institute of Technology, Pasadena, 1970, p. 228.
- [13] C. Everitt, T. Damour, K. Nordtvedt, R. Reinhard, "Historical perspective on testing the equivalence principle", *Adv. Space Res.* **32** (2003), no. 7, p. 1297-1300.
- [14] P. Touboul, M. Rodrigues, G. Métris, B. Tatry, "MICROSCOPE, testing the equivalence principle in space", *C. R. Acad. Sci., Paris IV* **2** (2001), no. 9, p. 1271-1286.
- [15] P. Touboul, G. Métris, V. Lebat, A. Robert, "The MICROSCOPE experiment, ready for the in-orbit test of the equivalence principle", *Class. Quantum Gravity* **29** (2012), no. 18, article ID 184010.
- [16] E. Hardy, A. Levy, M. Rodrigues, P. Touboul, G. Métris, "Validation of the in-flight calibration procedures for the MICROSCOPE space mission", *Adv. Space Res.* **52** (2013), no. 9, p. 1634-1646.
- [17] P. Touboul, G. Métris, M. Rodrigues, Y. André, Q. Baghi, J. Bergé, D. Boulanger, S. Bremer, R. Chhun, B. Christophe, V. Cipolla, T. Damour, P. Danto, H. Dittus, P. Fayet, B. Foulon, P.-Y. Guidotti, E. Hardy, P.-A. Huynh, C. Lämmerzahl, V. Lebat, F. Liorzou, M. List, I. Panet, S. Pires, B. Pouilloux, P. Prieur, S. Reynaud, B. Rievers, A. Robert, H. Selig, L. Serron, T. Sumner, P. Visser, "Space test of the equivalence principle: first results of the MICROSCOPE mission", *Class. Quantum Gravity* **36** (2019), no. 22, article ID 225006.
- [18] C. Fallet, M. Le Du, C. Pittet, P. Prieur, A. Torres, "First in orbit results from DEMETER", in *28th Annual AAS Control and Guidance Conference*, Univelt, San Diego, CA, 2005.
- [19] M. Le Du, J. Maureau, P. Prieur, "Myriade : an adaptative concept", in *5th ESA International Conference on Spacecraft Guidance, Navigation and Control Systems in Frascati*, ESA Publications Division, Oordwijk, 2002.
- [20] P. Prieur, T. Lienart, M. Rodrigues, P. Touboul, T. Denver, J. L. Jorgensen, A. M. Bang, G. Metris, "MICROSCOPE mission: on-orbit assessment of the drag-free and attitude control system", in *Paper presented at 31st International Symposium on Space Technology and Science (ISTS 2017), Matsuyama-Ehime, Japan*, 2017.
- [21] P. Touboul, B. Foulon, M. Rodrigues, J. P. Marque, "In orbit nano-g measurements, lessons for future space missions", *Aerosp. Sci. Technol.* **8** (2004), no. 5, p. 431-441.
- [22] J. Flury, S. Bettadpur, B. D. Tapley, "Precise accelerometry onboard the grace gravity field satellite mission", *Adv. Space Res.* **42** (2008), no. 8, p. 1414-1423.
- [23] J.-P. Marque, B. Christophe, B. Foulon, "Accelerometers of the GOCE mission: return of experience from one year of in-orbit", in *ESA Living Planet Symposium*, ESA Special Publication, vol. 686, 2010, p. 57.

- [24] R. Rummel, W. Yi, C. Stummer, "GOCE gravitational gradiometry", *J. Geod.* **85** (2011), p. 777-790.
- [25] E. Willemenot, P. Touboul, "On-ground investigation of space accelerometers noise with an electrostatic torsion pendulum", *Rev. Sci. Instrum.* **71** (2000), no. 1, p. 302-309.
- [26] P. Touboul, G. Métris, M. Rodrigues, Y. André, Q. Baghi, J. Bergé, D. Boulanger, S. Bremer, P. Carle, R. Chhun, B. Christophe, V. Cipolla, T. Damour, P. Danto, H. Dittus, P. Fayet, B. Foulon, C. Gageant, P-Y. Guidotti, D. Hagedorn, E. Hardy, P.-a. Huynh, H. Inchauspe, P. Kayser, S. Lala, C. Lämmerzahl, V. Lebat, P. Leseur, F. Liorzou, M. List, F. Löffler, I. Panet, B. Pouilloux, P. Prieur, A. Rebray, S. Reynaud, B. Rievers, A. Robert, H. Selig, L. Serron, T. Sumner, N. Tangy, P. Visser, "MICROSCOPE mission: first results of a space test of the equivalence principle", *Phys. Rev. Lett.* **119** (2017), no. 23, p. 231101-1-231101-7.